PLOS ONE

RESEARCH ARTICLE

Early localized alterations of the retinal inner plexiform layer in association with visual field worsening in glaucoma patients

Rukiye Aydın☯, Mine Barış☯, Ceren Durmaz-Engin, Lama A. Al-Aswad, Dana M. Blumberg, George A. Cioffi, Jeffrey M. Liebmann, Tongalp H. Tezel, Gülgün Tezel*

Department of Ophthalmology, Vagelos College of Physicians and Surgeons, Columbia University, New York, NY, United States of America

☯ These authors contributed equally to this work.
* gt2320@cumc.columbia.edu

Citation: Aydın R, Barış M, Durmaz-Engin C, Al-Aswad LA, Blumberg DM, Cioffi GA, et al. (2021) Early localized alterations of the retinal inner plexiform layer in association with visual field worsening in glaucoma patients. PLoS ONE 16(2): e0247401. https://doi.org/10.1371/journal.pone.0247401

Editor: Sanjoy Bhattacharya, Bascom Palmer Eye Institute, UNITED STATES

Received: October 29, 2020

Accepted: February 6, 2021

Published: February 25, 2021

Data Availability Statement: All relevant data are within the manuscript and its Supporting Information files.

Funding: G.T. is supported by a research grant from National Eye Institute (R01EY028153); Homer McK. Rees Scholarship in Glaucoma Research; and the AR and JR Peacock Trusts Research Grant. This study has also been supported in part by a National Eye Institute grant for Core Facilities for Vision Research (P30

Abstract

Glaucoma is a chronic neurodegenerative disease of the optic nerve and a leading cause of irreversible blindness, worldwide. While the experimental research using animal models provides growing information about cellular and molecular processes, parallel analysis of the clinical presentation of glaucoma accelerates the translational progress towards improved understanding, treatment, and clinical testing of glaucoma. Optic nerve axon injury triggers early alterations of retinal ganglion cell (RGC) synapses with function deficits prior to manifest RGC loss in animal models of glaucoma. For testing the clinical relevance of experimental observations, this study analyzed the functional correlation of localized alterations in the inner plexiform layer (IPL), where RGCs establish synaptic connections with retinal bipolar and amacrine cells. Participants of the study included a retrospective cohort of 36 eyes with glaucoma and a control group of 18 non-glaucomatous subjects followed for two-years. The IPL was analyzed on consecutively collected macular SD-OCT scans, and functional correlations with corresponding 10–2 visual field scores were tested using generalized estimating equations (GEE) models. The GEE-estimated rate of decrease in IPL thickness ($R = 0.36$, $P<0.001$) and IPL density ($R = 0.36$, $P<0.001$), as opposed to unchanged or increased IPL thickness or density, was significantly associated with visual field worsening at corresponding analysis locations. Based on multivariate logistic regression analysis, this association was independent from the patients' age, the baseline visual field scores, or the baseline thickness or alterations of retinal nerve fiber or RGC layers ($P>0.05$). These findings support early localized IPL alterations in correlation with progressing visual field defects in glaucomatous eyes. Considering the experimental data, glaucoma-related increase in IPL thickness/density might reflect dendritic remodeling, mitochondrial redistribution, and glial responses for synapse maintenance, but decreased IPL thickness/density might correspond to dendrite atrophy. The bridging of experimental data with clinical findings encourages further research along the translational path.

EY019007) and an unrestricted grant from Research to Prevent Blindness.

Competing interests: The authors declare that they have no competing interests.

Introduction

Glaucoma is a leading cause of blindness, which affects approximately 80 million people worldwide. This chronic neurodegenerative disease is characterized by the progressive loss of retinal ganglion cells (RGCs), optic nerve axons, and synapses in the retina and brain. Experimental evidence from animal models of glaucoma suggests that RGC dendrites, which are arborized in the inner plexiform layer (IPL) of the retina and establish synaptic connections with bipolar and amacrine cells, may present structural and functional alterations in earlier stages of the disease process prior to detectable loss of RGC somas. Early structural alterations in RGC dendrites, including the shrinkage and loss of dendritic branches [1–3], may lead to synaptic rearrangements [4–9]. Since synapse plasticity may allow rewiring, it has been suggested that early alterations in the RGC dendritic arbor provide a treatment window to recover synapse dysfunction and prevent further injury to RGCs in this blinding disease [10–12]. However, present observations and potential translational implications are based on animal models, and despite a few clinical studies [13–15], current understanding of IPL alterations in human glaucoma remains highly limited.

While the basic science research using animal models provides growing information about pathogenic processes of glaucomatous neurodegeneration, parallel studies aim to validate the experimental data by analysis of postmortem human tissues and analysis of the imaging-based clinical data from glaucoma patients. Undoubtedly, collaborative efforts of basic scientists and clinical researchers can speed the translation from bench-to-bedside and back for ultimate success in preventing blindness from glaucoma. In order to test the relevance of experimental observations to human glaucoma, this retrospective cohort study analyzed selected locations for glaucoma-related IPL alterations and their functional association. Morphological alterations of the IPL were analyzed using sequentially obtained macular spectral domain optical coherence tomography (SD-OCT) scans of glaucoma patients, and the functional correlation of imaging-based parameters was analyzed using visual field test results. Findings of this study that support the functional importance of early localized IPL alterations in glaucomatous eyes provide a translational path and encourage further research for improved understanding, treatment, and clinical testing of glaucoma.

Materials and methods

Study participants

The Institutional Review Board of Columbia University reviewed and approved this study. Informed patient consent was obtained from all participants, and the tenets of the Declaration of Helsinki were followed.

For testing the functional association of localized IPL alterations, this study enrolled a retrospective cohort of 36 patients with primary open-angle glaucoma, and a control group consisting of 18 non-glaucomatous subjects, followed for two years.

Our selection criteria required sequential high-quality SD-OCT scans (with a quality score of 7 or above, assessed by the signal strength in a 0 to 10 rating scale) obtained using the same device, and reliable visual field tests (with fixation losses $\leq$33%, false-positive and false-negative rates $\leq$15%) obtained using 10–2 standard automated perimetry (Humphrey visual field analyzer, Carl Zeiss Meditec Inc., Dublin, CA). The sequential retinal scans with approximately two-year apart (24±3 months) were obtained at high-definition (HD) 5-line raster mode with macular SD-OCT (Cirrus HD-OCT, Carl Zeiss Meditec Inc.). All scans were well-focused, well-centered and without blinking or movement artifacts or scan tilt. The mean±SD quality score of the scans was 8.74±0.99. All patients underwent 10–2 visual field testing at the same visits.

A glaucoma specialist followed all patients and their complete ophthalmic examination included the best-corrected visual acuity, the spherical equivalent refractive error, slit lamp examination, intraocular pressure measurement, central corneal thickness measurement, and dilated examination of the retina and optic disc. The same examinations were repeated at their control visits.

The glaucoma diagnosis was based on an intraocular pressure of greater than 22 mmHg by Goldmann applanation tonometry, characteristic optic disc appearance (diffuse or focal thinning of the rim), and an abnormal visual field test result obtained by 24–2 standard automated perimetry (Humphrey visual field analyzer, Carl Zeiss Meditec Inc.). All patients had open angles with no secondary causes of glaucoma. Studied patients were also required to have a best-corrected visual acuity $\geq$ 20/50, a refractive error between $\pm$5.0 diopters sphere and $\pm$3.0 diopters cylinder, and an axial length between 22 and 26 mm. Only one eye of each participant was included in the study. If both eyes of the glaucoma patients met the inclusion criteria, the eye with less advanced glaucoma was selected to allow the analysis of early alterations in the IPL.

Glaucoma patients or non-glaucomatous controls with any other ocular or neurological diseases that could affect structural or functional measurements were excluded from the study. Cataract that could affect imaging parameters and visual field sensitivities, or retinal diseases that could interfere with retinal image analysis, such as age-related macular degeneration, epiretinal membrane, or diabetic retinopathy, were also excluded. In addition, patients were excluded if they had a history of intraocular surgery or laser capsulotomy (except for uncomplicated cataract or glaucoma surgery before the initiation of study period).

Image analysis

Graphic files of high resolution horizontal 5-line raster scans (within a 6×1 mm^2 area) were imported into image analysis program (ImageJ, National Institutes of Health, Bethesda, Maryland). The analyzed imaging parameters included the thickness of retinal nerve fiber layer (RNFL), RGC layer (RGCL), and IPL, and densitometry-based reflectance intensity of IPL as shown in **Fig 1**.

After delineating the borders of RNFL, RGCL, and IPL (using the segmented line tool of ImageJ), the local structural thickness (in μm) was analyzed and averaged on the nasal and temporal sides at a distance of 1, 1.5, and 2 mm from the center of the macula (which corresponds to an angular spacing of approximately 3, 5, and 7^0 from the macula center).

In addition to local thickness measurements, the image analysis also included densitometry as a supplemental method to analyze alterations in the IPL-specific texture. Densitometry-based analysis included both linear densitometry and area densitometry. For the aim to supplement the analysis of association between localized structural and functional alterations, linear densitometry [16] analyzed the IPL in the same retinal locations (as described above for thickness measurements). In order to capture additional information reflecting the entire area analyzed, the IPL density was also analyzed in the area within 2 mm (approximately 7^0) from the macula center on the nasal and temporal sides of the OCT scans (shown in **Fig 1**). At the beginning of each analysis, a scale was set to measure the thickness in μm, and the plot profile option was chosen for analysis, which gives a two-dimensional graph of reflectance intensities along a line or an area selection. The mean value that reflects the grayscale level within the area under the curve was recorded as the density value (grayscale intensity value/μm^2).

In order to minimize imaging variability in sequentially obtained scans, we applied a normalization strategy to raw intensity data as previously described [17, 18]. The mean intensity of pixels within the IPL was therefore divided by the mean intensity of sub-IPL tissue

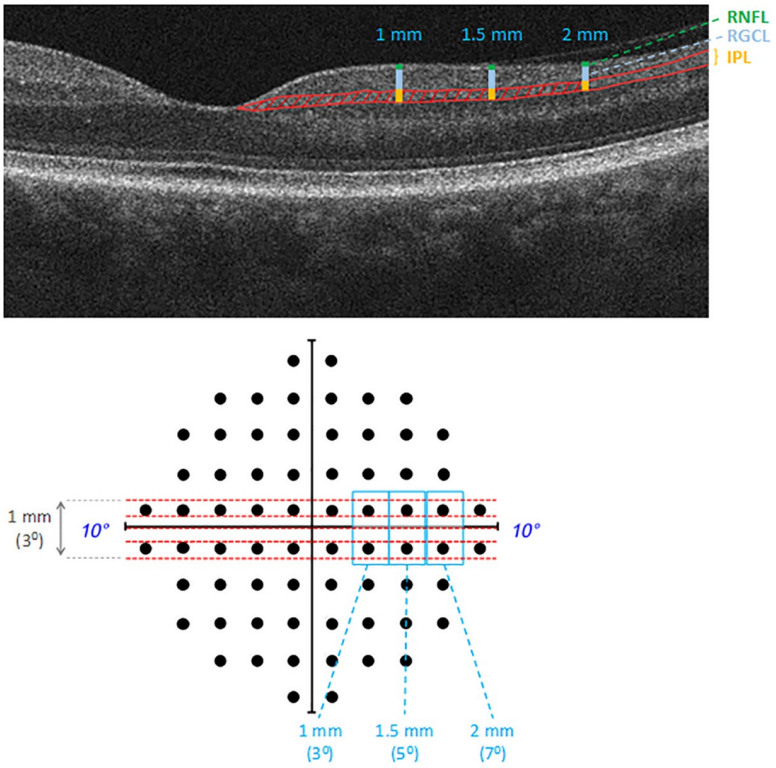

Fig 1. Studied imaging parameters of the IPL for testing functional associations. The imaging parameters analyzed on OCT scans included the thickness of the IPL (shown by yellow bar), RGCL (shown by blue bar), and RNFL (shown by green bar) on the nasal and temporal sides at a distance of 1, 1.5, and 2 mm from the center of the macula (shown is the nasal side). The IPL was also analyzed in the same retinal locations by linear densitometry. In addition, the IPL density was analyzed in the area within 2 mm (approximately 7^0) from the macula center on nasal and temporal sides of the OCT scans (red patterned area). For testing the functional association of these imaging parameters, corresponding total deviation values on 10–2 visual fields were used, including one below and one above the horizontal midline within 8^0 (shown in blue-colored boxes) on nasal and temporal fields. Red dashed lines illustrate the approximate position of 5-line raster scans that were obtained within a 6×1 mm^2 area, the vertical span of which (1 mm) corresponds to an angular spacing of approximately 3^0. The thickness and linear densitometry values obtained at 1, 1.5, and 2 mm from the macula center on these scans were tested against the average of total deviation scores at corresponding test points (approximately 3, 5, and 7^0); however, the area densitometry values were tested against the average of these values.

https://doi.org/10.1371/journal.pone.0247401.g001

(extending from one pixel below the posterior border of the IPL to the posterior border of the retinal pigment epithelium) and an intensity ratio (for linear and area densitometry scores, separately) was calculated for each scan. Note that the intensity scores of RNFL or RGCL were not used for normalization of the IPL grayscale intensity, because their glaucoma-related alterations are dependent on each other.

Manual image analysis was conducted by two researchers (RK and MB) masked to the patient's other data. Repeatability and reproducibility of image analysis were tested by calculating the coefficient of variation (CoV) and the coefficient of repeatability and reproducibility (COR). In addition, the intra-class correlation coefficient (ICC) was calculated using the two-way mixed-model for absolute agreement [19]. When assessed by the CoV, the intra-examiner and inter-examiner variabilities were 1.6±0.8% (95% confidence intervals, 1.1 to 2.1) and 2.6 ±0.9% (95% confidence intervals, 2.0 to 3.2), respectively (the COR were 2.2±1.2% and 3.7 ±1.8%, respectively). The ICC for absolute agreement of the two examiners was 0.992 (95% confidence intervals, 0.971–0.998) for IPL thickness, and 0.966 (95% confidence intervals,

0.862–0.992) for IPL density. Thus, the statistical measures showed good repeatability and reproducibility of the consecutive measurements of the same scans by two examiners. In addition, all of the measurements were repeated three times, and the mean values were used for statistical comparisons.

In order to assess scan-to-scan variability, the cohort of healthy eyes was tested three times within three consecutive weeks (and then yearly over two years). The CoV for density measurements in different scans was 6.9±1.2% (95% confidence intervals, 6.35 to 7.45); while the scan-to-scan variability for thickness measurements was 1.5±0.4% (95% confidence intervals, 1.25 to 1.75). The calculated variations (which reflect the reciprocal of the signal-to-noise ratio) support our utilized strategy as a repeatable measure of reflectance intensity.

For testing the functional correlation of imaging parameters, we used corresponding total deviation values (in dB) on 10–2 visual fields (**Fig 1**). In order to minimize challenges in the perfect pairing of corresponding imaging and functional parameters, studied test points were selected with particular attention to the approximate association of perimetry test points to anatomical location, functional architecture, and receptive fields of RGCs [20–22]. As explained in **Fig 1**, by considering *(A)* the position of 10–2 visual field test points (that are located at 1^0 from the horizontal and vertical midlines and then continue with 2^0 intervals); and *(B)* the vertical span of 5-line raster scans (1 mm, approximately 3^0), two test points (one below and one above the horizontal midline) were studied within 8^0 on nasal and temporal fields. The imaging parameters, including the thickness and linear densitometry values obtained at 1, 1.5, and 2 mm from the macula center (corresponding to approximately 3, 5, and 7^0) were tested against the average of total deviation values at corresponding two test points (at 3, 5, and 7^0). However, the area densitometry values (that were obtained from an area within 2 mm from the macula center on temporal and nasal sides) were tested against the average of total deviation values within 8^0 (at 3, 5, and 7^0) on the nasal and temporal fields (excluding the values at the center of the 10–2 fields by taking the displacement of RGCs in the macula into account [22]). Thus, selected test points provide optimum proximity for an appropriate structure-function analysis.

Statistical analysis

The statistical analysis was carried out using a statistics software, SPSS version 27 (IBM Corp., New York, NY). Group comparisons for demographic or intraocular pressure differences used the chi-square test for categorical variables and the t-test or the Mann-Whitney Rank Sum test for continuous variables. In order to account for potential association between the parameters analyzed at multiple locations in the same eye, all comparisons were performed using generalized estimating equations (GEE). The rate of change in imaging parameters and visual field scores over the follow-up was calculated by repeated-measures regression models under the GEE framework. For testing the functional association of IPL alterations, the GEE multivariate logistic model evaluated the effect of other variables on relative odds. A P value of less than 0.05 was considered statistically significant. All data are presented as mean±standard deviation accompanied by univariate or bivariate scatterplots when applicable.

Results

Demographic and clinical characteristics of the studied patients with glaucoma and non-glaucomatous controls are presented in **Table 1**. Based on 24–2 visual field scores, the baseline stage of glaucoma was mild (31%; mean deviation, <-5.00 dB), moderate (39%; mean deviation, -5.01 to -12.00 dB), or severe (31%; mean deviation, >-12.01 dB). Throughout the two-year follow-up, the elevated intraocular pressure in glaucoma patients (>22 mmHg at

Table 1. Demographic features and clinical characteristics of the study groups.

	Glaucoma	Control	Significance (P)
Number of eyes	36	18	
Age, year	68±11 (51 to 88)	66±6 (52 to 74)	0.4
Gender, female	16 (44%)	8 (44%)	1
24–2 Visual field mean deviation, dB	-9.05±10.85 (-1.65 to -26.83)	0.23±1.01 (2.06 to -1.12)	<0.001
<-5.00 dB	*11 (31%)*	*18 (100%)*	
-5.01–12.00 dB	*14 (39%)*	-	
>-12.00 dB	*11 (31%)*	-	
IOP, mmHg	12.83±3.09 (9 to 18)	12.78±2.69 (10 to 17)	0.9
Number of IOP-lowering medications	2.20±0.82 (1 to 3)	-	
Type of IOP-lowering medications			
alpha-adrenergic agonists	*15 (42%)*		
beta-adrenergic blockers	*14 (39%)*		
carbonic anhydrase inhibitors	*16 (44%)*		
prostaglandin analogs	*18 (50%)*		

Data are presented as mean±SD (range) when applicable.

https://doi.org/10.1371/journal.pone.0247401.t001

diagnosis) was under control by a combination of intraocular pressure-lowering topical medications, also presented in Table 1.

Similar analyses were run in the group of glaucoma patients and the control group of non-glaucomatous healthy individuals over the two-year follow-up. The data from image analysis of sequential macular scans and corresponding 10–2 visual fields (mean+SD) are summarized in Table 2. Presented in this table include 10–2 total deviation scores (dB) and baseline thickness of RNFL, RGCL, and IPL. Besides IPL thickness, two additional sets of data from densitometry-based analysis of IPL include linear densitometry (obtained at a distance of 1, 1.5, and 2 mm from the center of the macula on nasal and temporal sides) and area densitometry values (obtained from the area within 2 mm from macula center). Table 2 also presents the yearly progression rates of these structural and functional parameters, which were estimated by GEE. As expected, no prominent alteration was detected in non-glaucomatous controls, and their 10–2 total deviation scores remained no worse than -3.00 dB (P = 0.96) over the two-year follow-up.

Table 2. Summary of the data from sequential analysis of macular SD-OCT scans and visual fields.

	Baseline		Yearly Change (95% CI)	
	Control	Glaucoma	Control	Glaucoma *
Number of eyes	**18**	**36**	**18**	**36**
Retinal nerve fiber layer thickness (μm)	89.11±6.72	42.67±13.40	-0.14±0.08 (-0.30–0.20)	-0.95±0.25 (-1.43- -0.47)
Retinal ganglion cell layer thickness (μm)	91.98±5.58	47.16±13.24	-0.20±0.10 (-0.40- -0.01)	-0.94±0.14 (-1.22- -0.83)
Inner plexiform layer thickness (μm)	73.91±8.74	57.85±10.77	-0.16±0.58 (-1.11–0.79)	-1.23±0.90 (-2.99–0.54)
Inner plexiform layer linear density ratio	0.74±0.10	0.77±0.14	0.01±0.002 (0.001–0.01)	-0.03±0.01 (-0.06- -0.01)
Inner plexiform layer area density ratio	0.79±0.11	0.84±0.12	-0.004±0.08 (-0.14–0.12)	-0.04±0.08 (-0.17–0.10)
10–2 Visual field total deviation (dB)	1.18±2.12	-9.05±8.36	-0.17±0.08 (-0.32–0.02)	-0.67±0.43 (-1.51–0.16)

Data are presented as mean±SD. The rate of change over the follow-up was calculated under the generalized estimating equations (GEE) framework.

* The yearly change of the analyzed parameters were significant in the glaucoma group (P<0.001).

https://doi.org/10.1371/journal.pone.0247401.t002

Table 3. IPL alterations in glaucoma subgroups with different stages.

		IPL thickness (μm)		IPL linear density ratio	
Baseline 24–2 visual field scores	Number of eyes	Baseline	Two-year follow-up	Baseline	Two-year follow-up
<-5.00 dB	11	59.98±10.38	57.30±11.98	0.80±0.11	0.71±0.17
-5.01–12.00 dB	14	59.95±9.90	58.03±14.05	0.79±0.14	0.70±0.23
>-12.00 dB	11	53.75±10.74 *	50.92±15.17	0.71±0.14 *	0.62±0.25

Data are presented as mean±SD.

* The baseline thickness and density of the inner plexiform layer (IPL) were higher in the subgroup of severe glaucoma (>-12.00 dB) than other subgroups (P<0.001); however, the alterations in IPL thickness or density over the two-year follow-up were not different between subgroups (P>0.05).

https://doi.org/10.1371/journal.pone.0247401.t003

Table 3 presents the baseline and follow-up IPL data in the subgroups of glaucomatous eyes divided as mild, moderate, or severe based on 24–2 visual field scores at baseline. Although the baseline thickness and density of the IPL were significantly more advanced in eyes with severe glaucoma (P<0.001), the progression of these parameters was not significantly different between subgroups (P = 0.98, and P = 0.87, respectively).

Indeed, initial cross-sectional analysis of baseline parameters detected a significant correlation between RGCL and RNFL thicknesses (R = 0.92, P<0.001), RGCL thickness and visual field loss (R = 0.28, P<0.001), and RNFL thickness and visual field loss (R = 0.21, P = 0.002) in glaucomatous eyes. When analyzed cross-sectionally, the IPL thickness and density were also positively correlated (R = 0.75, P<0.001). In addition, both the IPL thickness and the linear density ratio showed a significant relationship to the stage of glaucomatous injury. As presented in Fig 2, the IPL thickness was significantly correlated with the RNFL thickness (R = 0.32, P<0.001), RGCL thickness (R = 0.35, P<0.001), and the total deviation scores of

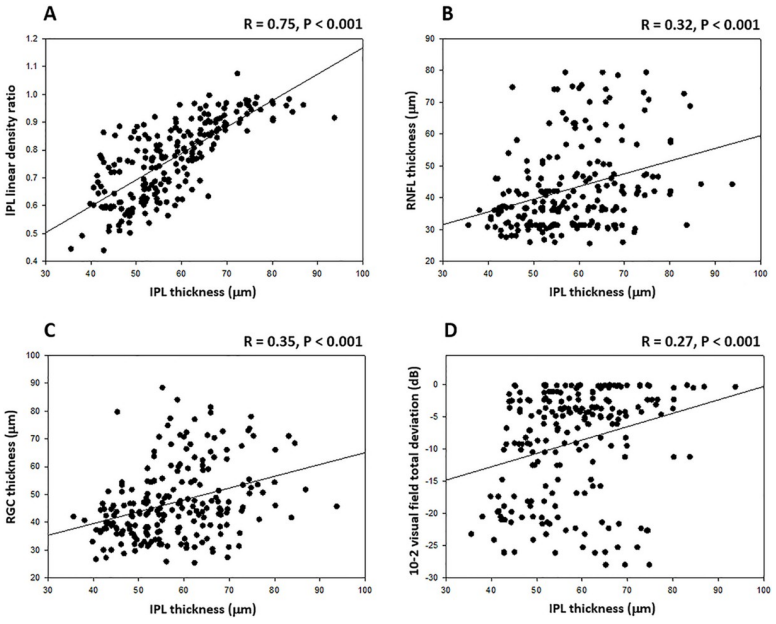

Fig 2. Baseline association of imaging parameters and visual field scores in patients with glaucoma. Presented include linear regression plots that show a significant relationship between the baseline values of IPL thickness and IPL linear density (**A**), IPL thickness and RNFL thickness (**B**), IPL thickness and RGCL thickness (**C**), and IPL thickness and 10–2 visual field total deviation (**D**).

https://doi.org/10.1371/journal.pone.0247401.g002

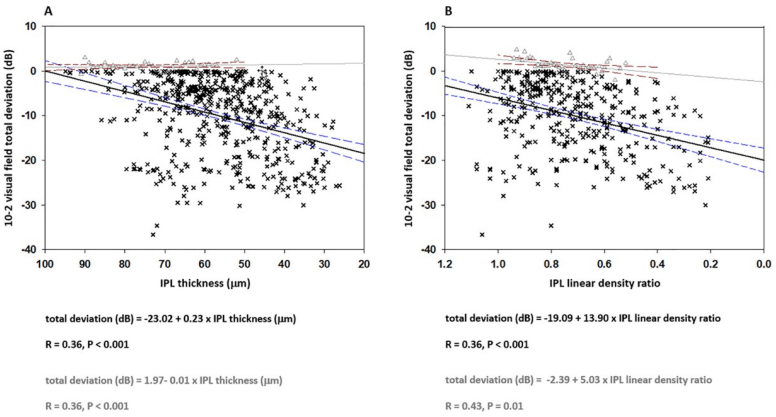

Fig 3. Sequential analysis of the association between IPL and visual field alterations in patients with glaucoma. Presented include the scatterplots showing a significant relationship between the alterations in IPL thickness and visual field scores (**A**), and alterations in IPL linear density and visual field scores (**B**) over the two-year follow-up. Dashed lines show the 95% confidence intervals for glaucomatous eyes (black solid line) and non-glaucomatous controls (gray solid line).

https://doi.org/10.1371/journal.pone.0247401.g003

10–2 visual fields (R = 0.27, P<0.001). Similarly, the IPL density presented a significant correlation with visual field scores (R = 0.89, P<0.001 for linear intensity ratios; and R = 0.78, P<0.001 for area intensity ratios). No association was detectable between the imaging parameters of IPL and the signal strength in analyzed SD-OCT scans (P>0.05).

When evaluated longitudinally, IPL alterations in the glaucomatous eyes exhibited a significant correlation with alterations in visual field scores. Fig 3 shows the IPL thickness, or IPL density, that were plotted against the visual field scores over the two-year follow-up. As presented in this figure, the alterations in IPL thickness (R = 0.36, P<0.001), or IPL density (R = 0.36, P<0.001), were significantly correlated with visual field worsening. When the rate of change in imaging and functional parameters was estimated by GEE, for every 10 μm decrease in IPL thickness per year, 10–2 visual field total deviation scores exhibited 2.3 dB decrease at corresponding locations. Similarly, the corresponding visual field scores worsened 1.39 dB for every 0.1 unit decrease in the IPL density. These associations detected between the decreasing IPL thickness (or IPL density) and the worsening of local visual field sensitivity scores were highly significant (P<0.001 for both IPL thickness and density).

However, the IPL alterations detected over the follow-up were not significantly associated with the change in RNFL thickness (R = 0.10, P = 0.11 for IPL thickness; R = 0.12, P = 0.09 for IPL density) or RGCL thickness (R = 0.12, P = 0.07 for IPL thickness; R = 0.05, P = 0.49 for IPL density) at corresponding spots in the studied glaucomatous eyes with treated intraocular pressure.

The alterations in IPL thickness, or IPL density, detected in the glaucomatous eyes were prominent at multiple analysis locations that exhibited decreased or increased values beyond the 95% confidence intervals of GEE-estimated progression rates. Comparison of the sequential image analysis data (from 216 analysis locations, including 1, 1.5, and 2 mm from the center of the macula on nasal and temporal sides) indicated that both the IPL thickness and the linear density ratio increased at 74 (34%) analysis locations out of 216; while only the IPL thickness increased at 3 (1%) or only the IPL density increased at 12 (6%) analysis locations. In contrast, at 67 analysis locations (31%), both the IPL thickness and the linear density ratio decreased, while only the IPL thickness decreased at 3 (1%) or only the IPL density decreased

at 31 (14%) analysis locations. Similarly, the area density of the IPL (analyzed within 2 mm from the center of the macula on nasal and temporal sides) increased at 24 out of 72 (33%) analysis locations, or decreased at 31 (43%) analysis locations. Fig 4 shows the distribution of analysis locations with or without IPL alterations. This figure also presents the patients' age, imaging parameters, and visual field sensitivity scores within these clusters that exhibited IPL alterations in different directions. Comparison of these groups with decreased IPL thickness and/or density to those with increased IPL thickness and/or density showed a significant difference in progression rates of visual field scores ($P<0.001$). The worsening of visual field scores during sequential analyses was more significant in the group with decreasing IPL thickness/density compared to the group of increasing IPL thickness/density. However, RNFL and RGCL thicknesses were not different ($P>0.05$) between the two groups of IPL alterations in different directions. Similar to alterations in the thickness and linear density of IPL, alterations in the IPL area density was also associated with alterations in visual field scores. The worsening of visual field scores was more significant in locations with a decreasing area density of the IPL, as opposed to the group with an increasing area density of the IPL ($P<0.001$) with no age differences ($P>0.05$). Fig 4 also shows vertical scatterplots for a better presentation of data distribution.

After detection of a significant association between the IPL thickness/density alterations and visual field worsening at corresponding test locations ($P<0.001$), additional covariates were added to the GEE model to determine for potential effects. Odds ratios were calculated for testing the impact of a set of variables (patients' age, baseline visual field scores, and the baseline values and the concurrent rate of change in other imaging parameters). Using the GEE multivariate logistic model, the association between the IPL thickness, or IPL density, decrease and the worsening of visual field scores was independent from the patients' age, the baseline thickness of RNFL, RGCL, or IPL, the baseline visual field scores, or the change in RNFL or RGCL thicknesses ($P>0.05$). Table 4A and 4B present the risk estimates for the functional association of IPL thickness and IPL density.

Fig 5 exemplifies localized IPL alterations and their functional correlation in sequentially analyzed glaucomatous eyes.

Discussion

This retrospective cohort study detected localized alterations in the IPL thickness and IPL density in association with progressing local visual field defects in glaucomatous eyes. Despite a number of previous studies that analyzed the RGCL-IPL complex [23–26], studies of isolated IPL remain limited, which include a few studies that were cross-sectional and only used the IPL thickness obtained with the automated segmentation software of SD-OCT. One of those studies found that the IPL thinning is associated with RGC injury [14]. This study reported that the IPL thickness (or the thickness of the RGCL-IPL complex) shows a stronger association with corresponding 24–2 visual field scores compared with the thickness of RNFL or RGCL. However, another study found that the IPL thickness is not as good as other parameters commonly tested for glaucoma diagnosis, such as thicknesses of the isolated macular RGCL or the RGCL complex [15]. More recently, cross-sectional analysis of the macular RGCL and IPL detected no evidence for preferential IPL thinning in glaucomatous eyes, but suggested that the distance from the fovea is an important determinant of IPL thickness [27]. Although these previous studies that specifically evaluated the IPL used automated segmentation, another cross-sectional study used manual segmentation and detected a significant decrease in RGCL and IPL thicknesses in severe glaucoma [13]. Our present study analyzed the IPL in manually segmented locations in consecutive scans that were obtained approximately two years apart

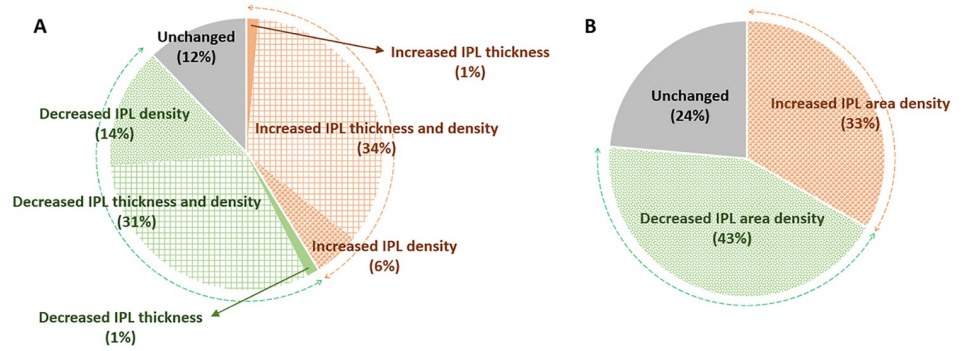

C

	Increased IPL thickness/density	Decreased IPL thickness/density	Significance (P) Increased vs Decreased	Unchanged IPL thickness/density	Significance (P) Decreased vs Unchanged (Increased vs Unchanged)
Number of spots (%)	89 (41.20)	101 (46.76)		26 (12.04)	
Age (year)	67±11	69±10	0.09	68±10	0.06 (0.67)
RNFL thickness change (μm/year)	-1.36±2.38	-1.25±2.39	0.75	-1.04±1.83	0.67 (0.52)
RGCL thickness change (μm/year)	-1.39±2.14	-0.99±1.92	0.22	-0.55±2.04	0.20 (0.08)
10-2 Visual field change (dB/year)	0.38±2.28	-2.62±2.86	<0.001	-0.29±0.56	<0.001 (<0.001)

	Increased IPL area density	Decreased IPL area density	Significance (P) Increased vs Decreased	Unchanged IPL thickness/density	Significance (P) Decreased vs Unchanged (Increased vs Unchanged)
Number of areas (%)	24 (33.33)	31 (43.06)		17 (23.61)	
Age (year)	68±12	71±9	0.5	67±10	0.21 (0.78)
10-2 Visual field change (dB/year)	0.84±0.38	-2.50±1.54	<0.001	-0.41±0.94	<0.001 (<0.001)

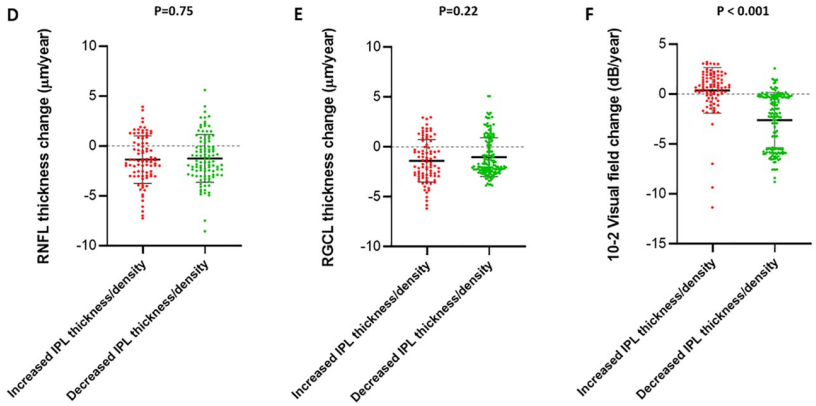

Fig 4. Distribution and associations of IPL alterations in patients with glaucoma. The pie graphs in panels A and B show the distribution of analysis locations with or without alterations in IPL imaging parameters over the two-year follow-up. These IPL alterations reflect those beyond the 95% confidence intervals of the change that was estimated by GEE. As shown in panel **A**, both the IPL thickness and the linear density increased at 74 (34%; red box-patterned area) analysis locations out of 216; while only the IPL thickness increased at 3 (1%; red area) or only the IPL density increased at 12 (6%; red dotted area) analysis locations. In contrast, at 67 analysis locations (31%; green box-patterned area), both the IPL thickness and the linear density decreased, while only the IPL thickness decreased at 3 (1%; green area) or only the IPL density decreased at 31 (14%; green dotted area) analysis locations. In 26 analysis locations (12%; gray area), the IPL thickness or density did not change significantly. As shown in panel **B,** the area density of the IPL (analyzed within 2 mm from the center of the macula on nasal and temporal sides) increased at 24 (33%; red area), decreased at 31 (43%, green area), or unchanged at 17 (24%; gray area) out of 72 analysis locations. Accompanying table **(C)** presents the RNFL thickness, RGCL thickness, and 10–2 visual field total deviation scores (mean±SD) for the analysis locations exhibiting increased (41%), decreased (47%), or unchanged (12%) IPL thickness and/or density, as shown in panel A. Vertical scatterplots show data distribution for RNFL thickness (**D**), RGCL thickness (**E**), and 10–2 visual field total deviation (**F**) in the subgroups with IPL alterations in different directions.

https://doi.org/10.1371/journal.pone.0247401.g004

and found a functional association. Based on the previous studies summarized above and present findings, it appears that the analysis of IPL may complement other imaging parameters for the diagnosis and monitoring of glaucoma. This clinical aspect highly motivates additional

Table 4.

A. Risk estimates for the association between the IPL thickness decrease and visual field worsening			
Parameters	**Odds Ratio**	**95% Confidence Interval**	Significance (P)
Age	1.03	0.75–1.31	0.35
Baseline RNFL thickness	0.98	0.96–1.00	0.16
Baseline RGCL thickness	0.97	0.95–0.99	0.18
Baseline IPL thickness	0.99	0.97–1.00	0.68
Baseline visual field scores	0.99	0.96–1.02	0.59
RNFL thickness change	0.95	0.93–0.96	0.32
RGCL thickness change	0.85	0.82–0.87	0.29
B. Risk estimates for the association between the IPL density decrease and visual field worsening			
Parameters	**Odds Ratio**	**95% Confidence Interval**	Significance (P)
Age	0.66	0.55–0.76	0.25
Baseline RNFL thickness	1.02	0.99–1.04	0.12
Baseline RGCL thickness	1.01	0.98–1.03	0.41
Baseline IPL thickness	0.99	0.96–1.02	0.66
Baseline visual field scores	1.01	0.98–1.04	0.58
RNFL thickness change	0.88	0.81–0.96	0.49
RGCL thickness change	0.63	0.52–0.74	0.48

To analyze the impacts of multiple variables on the association of IPL alterations with visual field worsening, odds ratios were calculated using the GEE multivariate logistic model. The significant association between decreasing IPL thickness/density and worsening of 10–2 visual field scores at corresponding test locations were independent from the patients' age, the baseline thickness of RNFL, RGCL, or IPL, the baseline visual field scores, or the change in RNFL or RGCL thicknesses ($P>0.05$). Odds ratio is given for a 1-unit change.

https://doi.org/10.1371/journal.pone.0247401.t004

studies to longitudinally investigate glaucoma-related IPL alterations. However, the main focus of our interest in this study remains as the clinical validation of experimental findings.

Besides alterations in retinal layer thicknesses, the potential contribution of various cellular and subcellular alterations to retinal reflectance changes is of growing interest. For example, microtubules have been shown to contribute to the reflectance of the RNFL [28]. A measurement of RNFL reflectance on SD-OCT scans has indicated glaucoma-related alterations in non-human primates [17] and humans [29, 30]. The glaucoma-related decrease in RNFL reflectance has also been found to precede the thinning of this layer in correlation with function loss in glaucomatous eyes [31, 32]. Relying on the RNFL reflectance intensity with potential to predict functional progression, the incorporation of thickness and reflectance information from SD-OCT has been suggested to improve the structure-function relation in glaucoma [18]. More recently, experimental OCT studies of the RGC5 cell line, retinal explants, and human eyes have suggested that texture measurements of the optical scatter signals derived from the subcellular network of organelles in RGCL and IPL have high potential for early clinical detection of RGC degeneration and guiding of treatment in glaucoma [33]. In fact, concentrated loss of RNFs within specific axon bundles, which leads to dark regions of RNF bundle defects, has very long been considered as one of the earliest clinical signs of glaucoma. Various other studies of glaucoma have utilized densitometry-based analysis for an evaluation of macular pigment in glaucomatous eyes [34], or an investigation of the origin of disc hemorrhages in glaucoma [35]. Notably, analysis of OCT images in age-related macular degeneration, together with high-resolution histology, has also indicated gliotic structures and mitochondria as important sources of reflectivity [36–38]. Since cellular and subcellular structures (such as mitochondria, cytoskeleton, microtubules) contribute to light scattering of the retina,

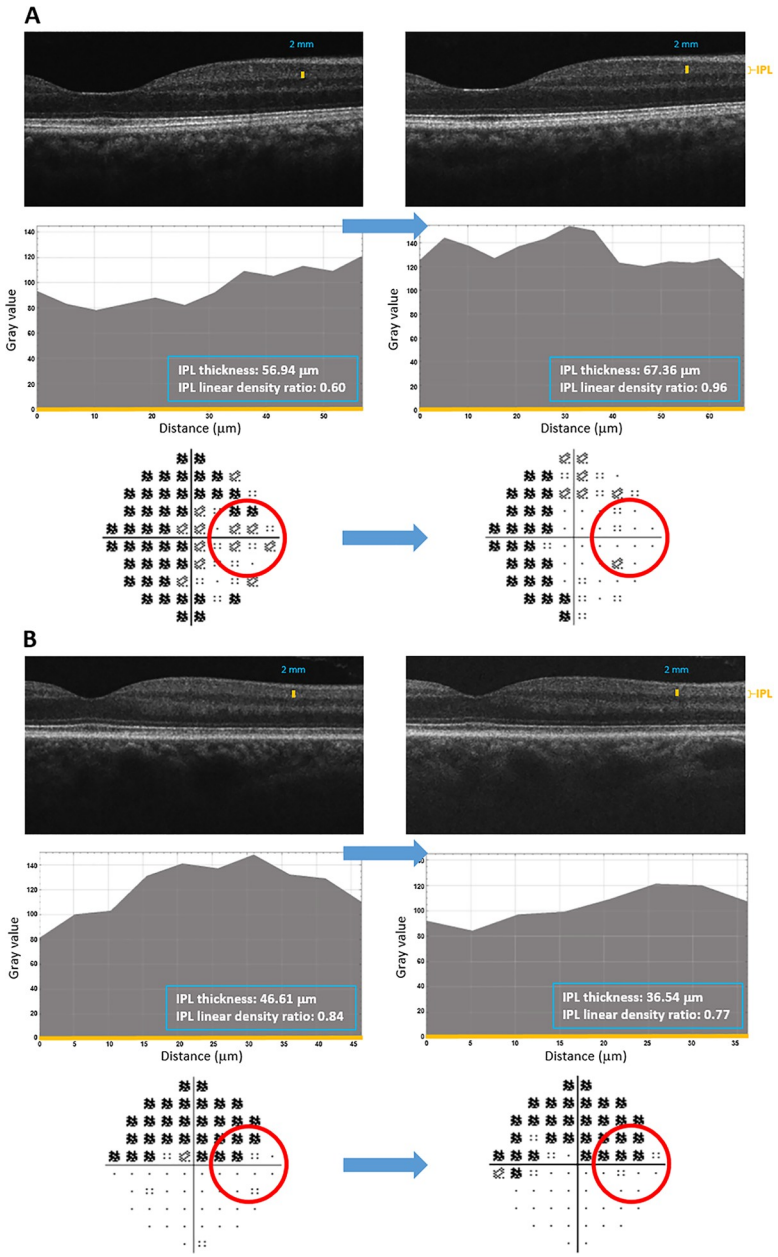

Fig 5. Sequential analysis of macular SD-OCT scans and 10–2 visual fields in patients with glaucoma. A. Temporal visual field points (red circle) corresponding to increased thickness (and density) of the IPL showed improvement. **B.** Temporal visual field points (red circle) corresponding to decreased thickness (and density) of the IPL showed worsening. The top rows in each panel show sequential macular SD-OCT scans. Middle rows in each panel show linear densitometry graphs obtained from the nasal side at 2 mm distance from the macula center. Bottom rows in each panel show 10–2 total deviation plots. The mean value of reflectance intensities that reflects the grayscale level within the area under the curve (grayscale intensity value/μm^2) was then normalized to minimize imaging variability in sequentially obtained scans (as described in our methodology). The numbers given in the blue box are the average IPL thickness and the average IPL intensity ratio calculated after normalization. The position where these data were obtained is marked with the yellow bar on SD-OCT scans. The thickness of the IPL corresponds to the X axis of the histograms (also shown in yellow color). Note that the localized alterations of IPL, such as decreased thickness (and density), were in correlation with progressing visual field defects at corresponding locations, most of which were clustered.

https://doi.org/10.1371/journal.pone.0247401.g005

our sequential image analysis in this study also included densitometry as an additional means to analyze glaucoma-related alterations in the IPL, the specific region of interest. For the aim to supplement the analysis of localized structural alterations by thickness measurements, our densitometry-based analysis included both linear densitometry (which is commonly applied in cataract studies [16] in the field of eye research, in addition to widespread applications in other systems) and area densitometry (which is commonly utilized in eye research studies). While the linear densitometry analyzed the IPL at specific locations (where layer thicknesses were measured), area densitometry aimed to capture additional information reflecting the entire area analyzed. Indeed, our reflectivity data (from linear and area densitometry) were in line with thickness measurements in correlation with the functional data.

Our findings indicated a significant relationship between localized structural alterations of the IPL (alterations in its thickness and density) and corresponding functional alterations on 10–2 visual fields (which provide higher detecting resolution than other types of perimetry [39]). As opposed to increasing thickness and/or density of the IPL, decreasing IPL thickness/density over the follow-up was found to be significantly associated with progressing visual field defects at corresponding locations (despite no prominent worsening in RNFL and RGCL thicknesses overall). One of the previous studies that analyzed the thickness of the RGCL-IPL complex in glaucoma patients similarly found a good correlation with the local loss of visual field sensitivity within approximately central 8˚ of fixation [21]. Another study that investigated the effect of glaucoma on different retinal layers also detected a thinner IPL in association with horizontal hemifield visual field defects [40].

It should be highlighted that our study had some limitations inherent to the retrospective study design and a relatively small group size. In order to minimize the potential sources of patient-related variability, we applied a strict eligibility criteria to select our study group of 36 eyes with primary open-angle glaucoma, in which localized imaging parameters and visual field scores were sequentially analyzed at three time points. With respect to the increasing chance of ocular and systemic health problems and the required treatments in this patient population, we considered that the inclusion of additional follow-up visits would further decrease the number of eyes fulfilling our selection criteria for this retrospective cohort study. We also thought that due to the chronic nature and asynchrony of neurodegeneration and dynamic processes of glial and healing responses in glaucoma, a two-year study period would provide clearer information about localized structure-function interaction (particularly for reflectance intensity that was utilized in addition to thickness measurements) without the cumulative addition of potential confounding impacts over a longer follow-up. Our careful set of criteria for patient selection should minimize many potential sources of sample variability and analysis error. However, the findings of this study should be further validated in prospective studies of larger and longer cohorts.

It is also important to clarify that since our study aimed to analyze the functional relevance of localized IPL alterations (but not to generate a structure-function map), selected locations on macular horizontal scans were analyzed against corresponding test points of 10–2 visual fields. However, there are common challenges of structure-function analysis, such as limitations in the perfect pairing of corresponding imaging and functional parameters, or the small stimulus size (standard size III stimulus corresponds to 0.43^0). To minimize these problems and allow the most feasible and appropriate analysis of structural and functional parameters with optimum proximity, we carefully selected test locations. Yet, due to individual, spatial, and temporal variability, additional studies are needed for further validation and expansion of the information by testing additional locations (such as arcuate damage areas) repeatedly over a longer study period. Evolving techniques of structure-function modeling should further improve the representation of corresponding structural and functional information for such

studies. Our densitometry-based analysis supplemented thickness measurements to support experimental observations of early IPL alterations with functional relevance. However, as we also discussed later below, whether intensity measurements may be useful as an additional clinical metric in the future should also be further studied.

Another important aspect to clarify relates to the challenges in assessing the glaucoma progression in imaging parameters due to measurement variability (as well as biological variability that results in individual differences in pathogenic processes). The high quality scores of the analyzed HD-OCT scans (7 or above as an inclusion criteria) that were obtained using the same device in consecutive visits, along with the good repeatability and reproducibility of manual image analysis, should minimize operator-related variability in this study. Besides avoiding off-axis fundus scanning or tilted images, analysis of macular horizontal scans (where tilting effect should be minimum), and exclusion of high myopic eyes (because myopia-related posterior segment pathology might cause position problems) should diminish the variability of retinal thickness measurements in tilted or axially stretched OCT images [41]. Concerning the imaging variability, although internal reflectivity promises useful information (and increasing resolution of SD-OCT scans makes its analysis possible), sequential comparison of pixel intensity values may be even more difficult than layer thickness measurements, because tissue reflectance varies between scans (due to differences in the exact focal plane or the quality of preretinal optics affecting light intensity). Even though we analyzed high quality scans, internal image processing (such as lossy compression of OCT scans and down sampling of graphic files) may only have minimal impact on thickness measurements (and help segmentation by clear contrast change), but may have more effect on the analysis of grayscale values. To minimize test-retest variability in pixel intensity and to better represent alterations in tissue-specific optical properties, we used a normalization strategy similar to that previously used for analysis of the RNFL reflectance intensity in glaucoma [18]. Our repeatability (as determined by the average per-eye CoV in healthy controls) was approximately 10%. The previously reported test-retest variability of the RNFL reflectance using the same measure was more than twice higher than the repeatability of IPL reflectance in our study [18]. This might be related to differences in the directionality of reflectance [42, 43] between the two retinal layers (since the RNFL contains more cylindrical structures, such as axons and their aligned cytoskeletal components), as well as equipment-related differences. We recognize that although we found a significant positive correlation between the IPL thickness and IPL density (thereby providing an internal control) and also detected a significant trend of correlation between the local alterations of IPL density and corresponding visual field scores, additional studies with methodological improvements are warranted to further verify and expand presented observations of the IPL reflectance. Our main conclusion that was based on the data derived from the multiple logistic regression analysis under the GEE framework were separately presented for the functional association of IPL thickness and IPL density changes (**Table 3**). Although alterations in IPL thickness were parallel to alterations in its density, the IPL thickness changes may be considered more robust for further discussion of our findings herein (compared to changes in density due to potential of the technical drawbacks noted).

Experimental studies of glaucoma using animal models have detected early structural alterations in RGC dendrites and synapses and accompanying function deficits prior to manifest RGC death [1–10, 44]. Neurons in the retina, similar to other brain neurons [45], have dendritic and synaptic plasticity [46, 47]. Although the number of synapses decrease as neurodegeneration progresses in ocular hypertensive animals, tissue repair and remodeling attempts are also evident prior to dendrite atrophy, synaptic pruning, and function loss. Unlike axons in the central nervous system, which are not regenerative, dendrites respond to injury, develop new dendritic branches, and expand in a larger field [48]. Experimental observations in ocular

hypertensive animals similarly suggest an increase in synaptic vesicle proteins and the number of immature synapses between RGCs and bipolar cells [49].

Findings of the present study may be considered supportive of these experimental observations. A prominent alteration we detected at multiple analysis locations was increasing thickness (and density) of the IPL before further RGC and RNF loss. Interestingly, visual field sensitivity scores appeared to be more stable in test locations exhibiting increased thickness (and density) of the IPL. We wonder whether imaging-based alterations in the IPL-specific texture in the glaucomatous eyes might possibly reflect the early intrinsic recovery responses detected in experimental models, such as dendritic remodeling, accompanying mitochondrial redistribution [50], and glial responses. With respect to mitochondria being critical to energy-demanding maintenance and function of synapses [51], altered mitochondrial dynamics (such as mitochondrial transport to synapse site and/or local biogenesis in dendrites) might possibly be related to the detected increase in IPL thickness (and density). Another cellular response in the glaucomatous retina is early microglial activation as evident in human glaucoma [52] and animal models [53, 54]. Therefore, migration of microglia to the IPL (or potential alterations of Müller glia, processes of which spread through the retina and envelop synapses) might also be linked to the increased IPL thickness (and density) we detected. Evidently, these glial cells may provide early neurotrophic and metabolic/ionic/extracellular buffering support (the latter being particularly attributed to Müller glia) to stressed neurons, and may promote tissue healing by eliminating the injured dendritic structures through scavenger and phagocytosing functions [55–57]. Thus, the glaucoma-related increase in IPL thickness (and density) might possibly reflect early cellular responses for tissue repair and dendrite remodeling. The protected visual field function with increased IPL thickness (and density) may also correspond to an early and transient axogenic response to boost RGC excitability to maintain visual signaling [58]. In contrary, insufficiency or withdrawal of adaptive responses lead to dendrite atrophy that would be expected to cause tissue thinning (and density decrease) in the IPL with function loss as we detected in association with progressing visual field defects. The reduced synaptic activity drives axon degeneration, further worsening the visual function.

It is also noteworthy that the intrinsic healing attempts may reflect a longer process prior to synaptic pruning and function loss in human glaucoma that is typically treated to lower intraocular pressure, unlike animal models. However, despite an effective control of intraocular pressure in the studied eyes, sequential analysis indicated progression of visual field defects (in association with IPL alterations) in many of the test locations. Hence, intrinsic efforts or extrinsic treatments (currently limited to intraocular pressure-lowering medications) may delay, but may not always prevent, further neuron injury. With respect to synaptic plasticity and rewiring capacity, early alterations in RGC dendrites may offer a window of opportunity for further neuroprotective treatments [10]. Indeed, experimental evidence from animal models of glaucoma supports the possibility of neuroprotection to recover injured dendrites and prevent further injury to RGCs [11, 12].

In summary, the presented observations in the glaucomatous human retina may provide a clinical correlation to recent experimental findings in animal models and support a relationship between IPL alterations (that may precede other structural alterations) and progression of local visual field defects. Additional work in larger patient groups is needed to analyze IPL alterations in different regions of the retina and to assess covariate effects on structural and functional parameters more closely. In addition to patients with glaucoma, longitudinal studies of ocular hypertensive patients with no manifest glaucoma can also help collect further information about the chronology and functional association of IPL alterations. Continuously evolving imaging techniques and structure-function models are expected to accelerate the speed of progress in the field, so that increasing information should help determine whether

early detection of IPL alterations in glaucomatous eyes may contribute to clinical testing of glaucoma (particularly to the emerging artificial intelligence-based diagnostic strategies). Growing knowledge gained from clinical observations should guide the interpretation of experimental findings and encourage further research towards improved treatment of this blinding disease.

Author Contributions

Conceptualization: Gülgün Tezel.

Data curation: Rukiye Aydın, Mine Barış, Ceren Durmaz-Engin, Gülgün Tezel.

Formal analysis: Tongalp H. Tezel, Gülgün Tezel.

Funding acquisition: Gülgün Tezel.

Investigation: Rukiye Aydın, Mine Barış, Ceren Durmaz-Engin, Gülgün Tezel.

Methodology: Gülgün Tezel.

Project administration: Gülgün Tezel.

Resources: Lama A. Al-Aswad, Dana M. Blumberg, George A. Cioffi, Jeffrey M. Liebmann, Tongalp H. Tezel, Gülgün Tezel.

Software: Gülgün Tezel.

Supervision: Gülgün Tezel.

Validation: Gülgün Tezel.

Visualization: Gülgün Tezel.

Writing – original draft: Gülgün Tezel.

Writing – review & editing: Gülgün Tezel.

References

1. Weber AJ, Kaufman PL, Hubbard WC. Morphology of single ganglion cells in the glaucomatous primate retina. Invest Ophthalmol Vis Sci. 1998; 39: 2304–2320. PMID: 9804139
2. Shou T, Liu J, Wang W, Zhou Y, Zhao K. Differential dendritic shrinkage of alpha and beta retinal ganglion cells in cats with chronic glaucoma. Invest Ophthalmol Vis Sci. 2003; 44: 3005–3010. https://doi.org/10.1167/iovs.02-0620 PMID: 12824245
3. Williams PA, Howell GR, Barbay JM, Braine CE, Sousa GL, John SW, et al. Retinal ganglion cell dendritic atrophy in DBA/2J glaucoma. PLoS One. 2013; 8: e72282. https://doi.org/10.1371/journal.pone.0072282 PMID: 23977271
4. Frankfort BJ, Khan AK, Tse DY, Chung I, Pang JJ, Yang Z, et al. Elevated intraocular pressure causes inner retinal dysfunction before cell loss in a mouse model of experimental glaucoma. Invest Ophthalmol Vis Sci. 2013; 54: 762–770. https://doi.org/10.1167/iovs.12-10581 PMID: 23221072
5. Della Santina L, Inman DM, Lupien CB, Horner PJ, Wong RO. Differential progression of structural and functional alterations in distinct retinal ganglion cell types in a mouse model of glaucoma. J Neurosci. 2013; 33: 17444–17457. https://doi.org/10.1523/JNEUROSCI.5461-12.2013 PMID: 24174678
6. Feng L, Zhao Y, Yoshida M, Chen H, Yang JF, Kim TS, et al. Sustained ocular hypertension induces dendritic degeneration of mouse retinal ganglion cells that depends on cell type and location. Invest Ophthalmol Vis Sci. 2013; 54: 1106–1117. https://doi.org/10.1167/iovs.12-10791 PMID: 23322576
7. Berry RH, Qu J, John SW, Howell GR, Jakobs TC. Synapse loss and dendrite remodeling in a mouse model of glaucoma. PLoS One. 2015; 10: e0144341. https://doi.org/10.1371/journal.pone.0144341 PMID: 26637126
8. El-Danaf RN, Huberman AD. Characteristic patterns of dendritic remodeling in early-stage glaucoma: evidence from genetically identified retinal ganglion cell types. J Neurosci. 2015; 35: 2329–2343. https://doi.org/10.1523/JNEUROSCI.1419-14.2015 PMID: 25673829

9. Ou Y, Jo RE, Ullian EM, Wong RO, Della Santina L. Selective vulnerability of specific retinal ganglion cell types and synapses after transient ocular hypertension. J Neurosci. 2016; 36: 9240–9252. https://doi.org/10.1523/JNEUROSCI.0940-16.2016 PMID: 27581463

10. Agostinone J, Di Polo A. Retinal ganglion cell dendrite pathology and synapse loss: Implications for glaucoma. Prog Brain Res. 2015; 220: 199–216. https://doi.org/10.1016/bs.pbr.2015.04.012 PMID: 26497792

11. Lindsey JD, Duong-Polk KX, Hammond D, Leung CK, Weinreb RN. Protection of injured retinal ganglion cell dendrites and unfolded protein response resolution after long-term dietary resveratrol. Neurobiol Aging. 2015; 36: 1969–1981. https://doi.org/10.1016/j.neurobiolaging.2014.12.021 PMID: 25772060

12. Lindsey JD, Duong-Polk KX, Hammond D, Chindasub P, Leung CK, Weinreb RN. Differential protection of injured retinal ganglion cell dendrites by brimonidine. Invest Ophthalmol Vis Sci. 2015; 56: 1789–1804. https://doi.org/10.1167/iovs.14-13892 PMID: 25634981

13. Moura AL, Raza AS, Lazow MA, De Moraes CG, Hood DC. Retinal ganglion cell and inner plexiform layer thickness measurements in regions of severe visual field sensitivity loss in patients with glaucoma. Eye (Lond). 2012; 26: 1188–1193. https://doi.org/10.1038/eye.2012.110 PMID: 22699978

14. Kim EK, Park HL, Park CK. Segmented inner plexiform layer thickness as a potential biomarker to evaluate open-angle glaucoma: Dendritic degeneration of retinal ganglion cell. PLoS One. 2017; 12: e0182404. https://doi.org/10.1371/journal.pone.0182404 PMID: 28771565

15. Chien JL, Ghassibi MP, Patthanathamrongkasem T, Abumasmah R, Rosman MS, Skaat A, et al. Glaucoma diagnostic capability of global and regional measurements of isolated ganglion cell layer and inner plexiform layer. J Glaucoma. 2017; 26: 208–215. https://doi.org/10.1097/IJG.0000000000000572 PMID: 27811573

16. Alberdi T, Mendicute J, Bascaran L, Barandika O, Ruiz-Ederra J. Anterior and posterior capsule densitometry levels after femtosecond laser-assisted cataract surgery. Int J Ophthalmol. 2018; 11: 623–628. https://doi.org/10.18240/ijo.2018.04.14 PMID: 29675381

17. Dwelle J, Liu S, Wang B, McElroy A, Ho D, Markey MK, et al. Thickness, phase retardation, birefringence, and reflectance of the retinal nerve fiber layer in normal and glaucomatous non-human primates. Invest Ophthalmol Vis Sci. 2012; 53: 4380–4395. https://doi.org/10.1167/iovs.11-9130 PMID: 22570345

18. Gardiner SK, Demirel S, Reynaud J, Fortune B. Changes in retinal nerve fiber layer reflectance intensity as a predictor of functional progression in glaucoma. Invest Ophthalmol Vis Sci. 2016; 57: 1221–1227. https://doi.org/10.1167/iovs.15-18788 PMID: 26978028

19. Bland JM, Altman DG. Statistical methods for assessing agreement between two methods of clinical measurement. Lancet. 1986; 1: 307–310. PMID: 2868172

20. Drasdo N, Millican CL, Katholi CR, Curcio CA. The length of Henle fibers in the human retina and a model of ganglion receptive field density in the visual field. Vision Res. 2007; 47: 2901–2911. https://doi.org/10.1016/j.visres.2007.01.007 PMID: 17320143

21. Raza AS, Cho J, de Moraes CG, Wang M, Zhang X, Kardon RH, et al. Retinal ganglion cell layer thickness and local visual field sensitivity in glaucoma. Arch Ophthalmol. 2011; 129: 1529–1536. https://doi.org/10.1001/archophthalmol.2011.352 PMID: 22159673

22. Hood DC, Raza AS, de Moraes CG, Odel JG, Greenstein VC, Liebmann JM, et al. Initial arcuate defects within the central 10 degrees in glaucoma. Invest Ophthalmol Vis Sci. 2011; 52: 940–946. https://doi.org/10.1167/iovs.10-5803 PMID: 20881293

23. Mwanza JC, Durbin MK, Budenz DL, Sayyad FE, Chang RT, Neelakantan A, et al. Glaucoma diagnostic accuracy of ganglion cell-inner plexiform layer thickness: comparison with nerve fiber layer and optic nerve head. Ophthalmology. 2012; 119: 1151–1158. https://doi.org/10.1016/j.ophtha.2011.12.014 PMID: 22365056

24. Jeoung JW, Choi YJ, Park KH, Kim DM. Macular ganglion cell imaging study: glaucoma diagnostic accuracy of spectral-domain optical coherence tomography. Invest Ophthalmol Vis Sci. 2013; 54: 4422–4429. https://doi.org/10.1167/iovs.12-11273 PMID: 23722389

25. Hammel N, Belghith A, Weinreb RN, Medeiros FA, Mendoza N, Zangwill LM. Comparing the rates of retinal nerve fiber layer and ganglion cell-inner plexiform layer loss in healthy eyes and in glaucoma eyes. Am J Ophthalmol. 2017; 178: 38–50. https://doi.org/10.1016/j.ajo.2017.03.008 PMID: 28315655

26. Lee WJ, Kim YK, Park KH, Jeoung JW. Trend-based analysis of ganglion cell-inner plexiform layer thickness changes on optical coherence tomography in glaucoma progression. Ophthalmology. 2017; 124: 1383–1391. https://doi.org/10.1016/j.ophtha.2017.03.013 PMID: 28412067

27. Moghimi S, Fatehi N, Nguyen AH, Romero P, Caprioli J, Nouri-Mahdavi K. Relationship of the Macular Ganglion Cell and Inner Plexiform Layers in Healthy and Glaucoma Eyes. Transl Vis Sci Technol. 2019; 8: 27. https://doi.org/10.1167/tvst.8.5.27 PMID: 31637107

28. Huang XR, Knighton RW, Cavuoto LN. Microtubule contribution to the reflectance of the retinal nerve fiber layer. Invest Ophthalmol Vis Sci. 2006; 47: 5363–5367. https://doi.org/10.1167/iovs.06-0451 PMID: 17122125

29. Vermeer KA, van der Schoot J, Lemij HG, de Boer JF. RPE-normalized RNFL attenuation coefficient maps derived from volumetric OCT imaging for glaucoma assessment. Invest Ophthalmol Vis Sci. 2012; 53: 6102–6108. https://doi.org/10.1167/iovs.12-9933 PMID: 22893674

30. Liu S, Wang B, Yin B, Milner TE, Markey MK, McKinnon SJ, et al. Retinal nerve fiber layer reflectance for early glaucoma diagnosis. J Glaucoma. 2014; 23: e45–52. https://doi.org/10.1097/IJG.0b013e31829ea2a7 PMID: 23835671

31. Pons ME, Ishikawa H, Gurses-Ozden R, Liebmann JM, Dou HL, Ritch R. Assessment of retinal nerve fiber layer internal reflectivity in eyes with and without glaucoma using optical coherence tomography. Arch Ophthalmol. 2000; 118: 1044–1047. https://doi.org/10.1001/archopht.118.8.1044 PMID: 10922196

32. Huang XR, Zhou Y, Kong W, Knighton RW. Reflectance decreases before thickness changes in the retinal nerve fiber layer in glaucomatous retinas. Invest Ophthalmol Vis Sci. 2011; 52: 6737–6742. https://doi.org/10.1167/iovs.11-7665 PMID: 21730345

33. Morgan JE, Tribble J, Fergusson J, White N, Erchova I. The optical detection of retinal ganglion cell damage. Eye (Lond). 2017; 31: 199–205. https://doi.org/10.1038/eye.2016.290 PMID: 28060357

34. Siah WF, Loughman J, O'Brien C. Lower macular pigment optical density in foveal-involved glaucoma. Ophthalmology. 2015; 122: 2029–2037. https://doi.org/10.1016/j.ophtha.2015.06.028 PMID: 26249732

35. Chou JC, Cousins CC, Miller JB, Song BJ, Shen LQ, Kass MA, et al. Fundus densitometry findings suggest optic disc hemorrhages in primary open-angle glaucoma have an arterial origin. Am J Ophthalmol. 2018; 187: 108–116. https://doi.org/10.1016/j.ajo.2017.12.024 PMID: 29330062

36. Litts KM, Wang X, Clark ME, Owsley C, Freund KB, Curcio CA, et al. Exploring photoreceptor reflectivity through multimodal imaging of outer retinal tubulation in advanced age-related macular degeneration. Retina. 2017; 37: 978–988. https://doi.org/10.1097/IAE.0000000000001265 PMID: 27584549

37. Dolz-Marco R, Litts KM, Tan ACS, Freund KB, Curcio CA. The evolution of outer retinal tubulation, a neurodegeneration and gliosis prominent in macular diseases. Ophthalmology. 2017; 124: 1353–1367. https://doi.org/10.1016/j.ophtha.2017.03.043 PMID: 28456420

38. Litts KM, Zhang Y, Freund KB, Curcio CA. Optical coherence tomography and histology of age-related macular degeneration support mitochondria as reflectivity sources. Retina. 2018; 38: 445–461. https://doi.org/10.1097/IAE.0000000000001946 PMID: 29210936

39. De Moraes CG, Hood DC, Thenappan A, Girkin CA, Medeiros FA, Weinreb RN, et al. 24–2 visual fields miss central defects shown on 10–2 tests in glaucoma suspects, ocular hypertensives, and early glaucoma. Ophthalmology. 2017; 124: 1449–1456. https://doi.org/10.1016/j.ophtha.2017.04.021 PMID: 28551166

40. Vianna JR, Butty Z, Torres LA, Sharpe GP, Hutchison DM, Shuba LM, et al. Outer retinal layer thickness in patients with glaucoma with horizontal hemifield visual field defects. Br J Ophthalmol. 2019; 103: 1217–1222. https://doi.org/10.1136/bjophthalmol-2018-312753 PMID: 30385436

41. Uji A, Abdelfattah NS, Boyer DS, Balasubramanian S, Lei J, Sadda SR. Variability of retinal thickness measurements in tilted or stretched optical coherence tomography images. Transl Vis Sci Technol. 2017; 6: 1–10. https://doi.org/10.1167/tvst.6.2.1 PMID: 28299239

42. Knighton RW, Huang XR. Directional and spectral reflectance of the rat retinal nerve fiber layer. Invest Ophthalmol Vis Sci. 1999; 40: 639–647. PMID: 10067967

43. Huang XR, Knighton RW, Feuer WJ, Qiao J. Retinal nerve fiber layer reflectometry must consider directional reflectance. Biomed Opt Express. 2016; 7: 22–33. https://doi.org/10.1364/BOE.7.000022 PMID: 26819814

44. Pang JJ, Frankfort BJ, Gross RL, Wu SM. Elevated intraocular pressure decreases response sensitivity of inner retinal neurons in experimental glaucoma mice. Proc Natl Acad Sci U S A. 2015; 112: 2593–2598. https://doi.org/10.1073/pnas.1419921112 PMID: 25675503

45. Tailby C, Wright LL, Metha AB, Calford MB. Activity-dependent maintenance and growth of dendrites in adult cortex. Proc Natl Acad Sci U S A. 2005; 102: 4631–4636. https://doi.org/10.1073/pnas.0402747102 PMID: 15767584

46. Lewis GP, Linberg KA, Fisher SK. Neurite outgrowth from bipolar and horizontal cells after experimental retinal detachment. Invest Ophthalmol Vis Sci. 1998; 39: 424–434. PMID: 9478003

47. Fisher SK, Lewis GP, Linberg KA, Verardo MR. Cellular remodeling in mammalian retina: results from studies of experimental retinal detachment. Prog Retin Eye Res. 2005; 24: 395–431. https://doi.org/10.1016/j.preteyeres.2004.10.004 PMID: 15708835

48. Papadopoulos CM, Tsai SY, Alsbiei T, O'Brien TE, Schwab ME, Kartje GL. Functional recovery and neuroanatomical plasticity following middle cerebral artery occlusion and IN-1 antibody treatment in the adult rat. Ann Neurol. 2002; 51: 433–441. https://doi.org/10.1002/ana.10144 PMID: 11921049

49. Park HY, Kim JH, Park CK. Alterations of the synapse of the inner retinal layers after chronic intraocular pressure elevation in glaucoma animal model. Mol Brain. 2014; 7: 53–64. https://doi.org/10.1186/s13041-014-0053-2 PMID: 25116810

50. Tribble JR, Vasalauskaite A, Redmond T, Young RD, Hassan S, Fautsch MP, et al. Midget retinal ganglion cell dendritic and mitochondrial degeneration is an early feature of human glaucoma. Brain Commun. 2019; 1: fcz035. https://doi.org/10.1093/braincomms/fcz035 PMID: 31894207

51. Ito YA, Di Polo A. Mitochondrial dynamics, transport, and quality control: A bottleneck for retinal ganglion cell viability in optic neuropathies. Mitochondrion. 2017; 36: 186–192. https://doi.org/10.1016/j.mito.2017.08.014 PMID: 28866056

52. Tezel G, Chauhan BC, LeBlanc RP, Wax MB. Immunohistochemical assessment of the glial mitogen-activated protein kinase activation in glaucoma. Invest Ophthalmol Vis Sci. 2003; 44: 3025–3033. https://doi.org/10.1167/iovs.02-1136 PMID: 12824248

53. Naskar R, Wissing M, Thanos S. Detection of early neuron degeneration and accompanying microglial responses in the retina of a rat model of glaucoma. Invest Ophthalmol Vis Sci. 2002; 43: 2962–2968. PMID: 12202516

54. Bosco A, Steele MR, Vetter ML. Early microglia activation in a mouse model of chronic glaucoma. J Comp Neurol. 2011; 519: 599–620. https://doi.org/10.1002/cne.22516 PMID: 21246546

55. Howell GR, Macalinao DG, Sousa GL, Walden M, Soto I, Kneeland SC, et al. Molecular clustering identifies complement and endothelin induction as early events in a mouse model of glaucoma. J Clin Invest. 2011; 121: 1429–1444. https://doi.org/10.1172/JCI44646 PMID: 21383504

56. Williams PA, Tribble JR, Pepper KW, Cross SD, Morgan BP, Morgan JE, et al. Inhibition of the classical pathway of the complement cascade prevents early dendritic and synaptic degeneration in glaucoma. Mol Neurodegener. 2016; 11: 26–39. https://doi.org/10.1186/s13024-016-0091-6 PMID: 27048300

57. Vecino E, Rodriguez FD, Ruzafa N, Pereiro X, Sharma SC. Glia-neuron interactions in the mammalian retina. Prog Retin Eye Res. 2016; 51: 1–40. https://doi.org/10.1016/j.preteyeres.2015.06.003 PMID: 26113209

58. Risner ML, Pasini S, Cooper ML, Lambert WS, Calkins DJ. Axogenic mechanism enhances retinal ganglion cell excitability during early progression in glaucoma. Proc Natl Acad Sci U S A. 2018; 115: E2393–E2402. https://doi.org/10.1073/pnas.1714888115 PMID: 29463759